

# Self-Assembly of Heterosupramolecules

Lucy Cusack, S. Nagaraja Rao, John Wenger, and Donald Fitzmaurice\*

Department of Chemistry, University College Dublin, Dublin 4, Ireland

Received August 26, 1996<sup>®</sup>

TiO<sub>2</sub> nanocrystallites are prepared by hydrolysis of titanium tetraisopropoxide in the presence of *N,N*-2,6-pyridinediylbis[undecamide]. The latter stabilizes the resulting semiconductor sol and provides sites at the surface of a nanocrystallite for selective binding of a uracil derivative by complementary hydrogen bonding. Addition of 6-(*N*-tridecylundecamido)methyluracil results in self-assembly of a heterosupramolecule subsequently characterized by <sup>1</sup>H NMR and FT-IR spectroscopies.

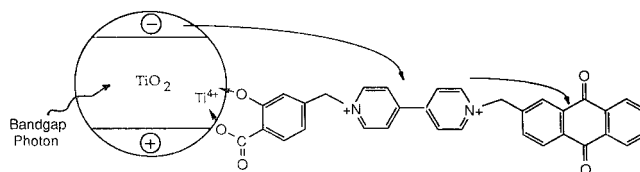
## Introduction

Conventionally, a supermolecule possesses properties that are not a simple superposition of those of its noncovalently linked molecular components.<sup>1</sup> Increasingly however, this term is applied to covalently linked molecular components provided, as above, identifiable supramolecular properties exist.<sup>2</sup> Nevertheless, an advantage of supermolecules containing noncovalently linked molecular components remains their potential for self-assembly.<sup>3,4</sup>

Supermolecules possessing suitable molecular components, whether covalently or noncovalently linked, may self-organize.<sup>5</sup> In principle, addressable function and the prospect of useful molecular-scale devices are consequences of self-organization.<sup>6</sup> In practice, progress toward the latter end has been limited by the stringent requirements that must be met by such devices: First, that they function at a supramolecular level within an assembly; second, that the function of each constituent supermolecule can be modulated independently; third, that the state of modulation of each supermolecule can be determined, and finally, that the resulting device meet speed, reliability, and cost specifications.

In respect of function modulation in molecular-scale devices, recent work directed toward development of a heterosupramolecular chemistry may offer new opportunities.<sup>7</sup> Briefly, upon replacing a molecular com-

Scheme 1



ponent in a supermolecule by a condensed phase component, a heterosupramolecule is formed. By analogy with supramolecular chemistry, identifiable heterosupramolecular properties exist. As for supermolecules, addressability is a consequence of organization. Uniquely however, because heterosupramolecules possess a condensed phase component, organization may yield an intrinsic substrate capable of modulating function and of providing information concerning modulation state.

The heterosupramolecule shown in Scheme 1 consists of a TiO<sub>2</sub> nanocrystallite coordinatively linked via a salicylic acid dianion to a viologen and anthraquinone moiety.<sup>7</sup> The latter are covalently linked by methylene spacers. The associated heterosupramolecular function is light-induced vectorial electron flow. Organization yields an intrinsic semiconductor substrate through which modulation of light-induced vectorial electron flow has proved possible.

As stated, a significant advantage of supermolecules containing noncovalently linked molecular components is their potential for self-assembly.<sup>3,4</sup> To date, however, only heterosupramolecules containing covalently linked condensed phase and molecular components have been prepared. In this context, we report recent work directed toward the noncovalent linkage of condensed phase and molecular components, i.e., the self-assembly of heterosupramolecules.

Specifically, TiO<sub>2</sub> nanocrystallites are prepared by hydrolysis of titanium tetraisopropoxide in the presence of *N,N*-2,6-pyridinediylbis[undecamide]. The latter stabilizes the resulting semiconductor sol and provides sites at the surface of a nanocrystallite for selective binding of a uracil derivative by complementary hydrogen bonding. Subsequent addition of 6-(*N*-tridecylundecamido)methyluracil results in self-assembly of the heterosupramolecule shown in Scheme 2. This heterosupramolecule has been the subject of detailed characterization by <sup>1</sup>H NMR and FT-IR spectroscopies. Some implications and possible applications of these findings are considered.

\* To whom correspondence should be addressed.

<sup>®</sup> Abstract published in *Advance ACS Abstracts*, November 1, 1996.

(1) (a) Lehn, J.-M. *Angew. Chem., Int. Ed. Engl.* **1988**, *27*, 89. (b) Cram, D. J. *Angew. Chem., Int. Ed. Engl.* **1988**, *27*, 1009. (c) Pederson, C. J. *Angew. Chem., Int. Ed. Engl.* **1988**, *27*, 1021. (d) Lehn, J.-M. *Supramolecular Chemistry*; VCH: New York, 1995.

(2) Balzani, V.; Scandola, F. *Supramolecular Photochemistry*; Ellis Horwood: New York, 1991; Chapter 3.

(3) (a) Lehn, J. M. *Angew. Chem., Int. Ed. Engl.* **1990**, *29*, 1304. (b) Philp, D.; Stoddart, J. F. *Synlett* **1991**, 445. (c) Lindsey, J. S. *New J. Chem.* **1991**, *15*, 153. (d) Whitesides, G. M.; Mathias, J. P.; Seto, C. T. *Science* **1991**, *254*, 1312.

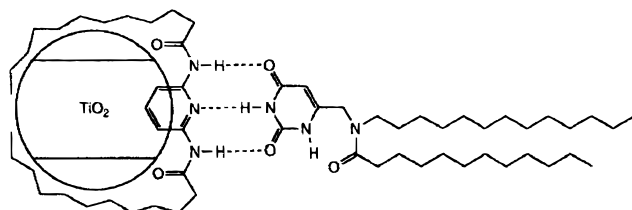
(4) (a) Whitesides, G. M.; Simanek, E. E.; Mathias, J. P.; Seto, C. T.; Chin, D. N.; Mammen, M.; Gordon, D. M. *Acc. Chem. Res.* **1995**, *28*, 37. (b) Lehn, J.-M. *Supramolecular Chemistry*; VCH: New York, 1995; Chapter 9.

(5) (a) Ringsdorf, H.; Schlarb, B.; Venzmer, J. *Angew. Chem., Int. Ed. Engl.* **1988**, *27*, 113. (b) Ahlers, M.; Muller, W.; Reichert, A.; Ringsdorf, H.; Venzmer, J. *Angew. Chem., Int. Ed. Engl.* **1990**, *29*, 1269.

(6) (a) Ashwell, G. *Molecular Electronics*; Wiley: New York, 1992. (b) *An Introduction to Molecular Electronics*; Petty, M., Bryce, M., Bloor, D., Eds.; Arnold: London, 1995.

(7) (a) Marguerettaz, X.; O'Neill, R.; Fitzmaurice, D. *J. Am. Chem. Soc.* **1994**, *116*, 2628. (b) Marguerettaz, X.; Fitzmaurice, D. *J. Am. Chem. Soc.* **1994**, *116*, 5017. (c) Marguerettaz, X.; Redmond, G.; S. Nagaraja Rao; Fitzmaurice, D. *Chem. Eur. J.* **1996**, *2*, 420.

Scheme 2



## Experimental Section

**Synthesis of Condensed Phase Components.**  $\text{TiO}_2$  nanocrystallites were prepared, following the method of Kotov et al.,<sup>8</sup> by arrested hydrolysis of titanium tetraisopropoxide. Briefly, titanium tetraisopropoxide (12.5  $\mu\text{L}$  in 2 mL of dry deuteriochloroform) was added to (8 mL) of deuteriochloroform containing added water (2  $\mu\text{L}$ ). The above addition was made under nitrogen during 3 h in the presence of added cetyltrimethylammoniumbromide (15 mg) or *N,N*-2,6-pyridinediylbis[undecamide] (20 mg) stabilizers. The resulting stable sol was characterized by UV-vis absorption spectroscopy and by transmission electron microscopy (TEM). All optical absorption spectra were recorded using a Hewlett-Packard 8452A diode array spectrophotometer. TEMs were recorded using a JEOL 2000 FX TEMSCAN. The observed onset for absorption and average crystallite diameter of 360 nm and  $22 \pm 2$  Å, respectively, are in good agreement with previously reported values.<sup>8</sup>

**Synthesis of Molecular Components.** Molecular components were prepared following methods previously reported by Lehn and co-workers.<sup>9</sup> Subsequent characterization was by elemental analysis and  $^1\text{H}$  NMR.

Calculated for *N,N*-2,6-pyridinediylbis[acetamide] ( $\text{C}_9\text{H}_{11}\text{N}_3\text{O}_2$ , **I**): C, 55.98; H, 5.74; N, 21.75. Found: C, 55.95; H, 5.74; N, 21.76.  $^1\text{H}$  NMR ( $\text{CDCl}_3$ )  $\delta$  2.20 (s, 6H), 7.61 (s, 2H), 7.73 (t, 1H,  $J = 8.2$  Hz), 7.86 (d, 2H,  $J = 8.2$  Hz).

Calculated for *N,N*-2,6-pyridinediylbis[undecamide] ( $\text{C}_{29}\text{H}_{51}\text{N}_3\text{O}_2$ , **II**): C, 73.53; H, 10.85; N, 8.87. Found: C, 73.60; H, 10.64; N, 8.91.  $^1\text{H}$  NMR ( $\text{CDCl}_3$ )  $\delta$  0.88 (t, 6H,  $J = 7.0$  Hz), 1.25–1.74 (m, 36H), 2.36 (t, 4H,  $J = 7.6$  Hz), 7.52 (s, 2H), 7.69 (t, 1H,  $J = 8.2$  Hz), 7.88 (d, 2H,  $J = 8.2$  Hz).

Calculated for 6-(*N*-tridecylamino)methyluracil ( $\text{C}_{18}\text{H}_{33}\text{N}_3\text{O}_2$ , **III**): C, 66.83; H, 10.28; N, 12.99. Found: C, 66.64; H, 10.26; N, 12.93.  $^1\text{H}$  NMR ( $\text{CDCl}_3$ )  $\delta$  0.88 (t, 3H,  $J = 6.6$  Hz), 1.26–1.86 (m, 22H), 2.56 (t, 2H,  $J = 7.1$  Hz), 3.61 (s, 2H), 5.52 (s, 1H), 8.32 (s, 2H, br).

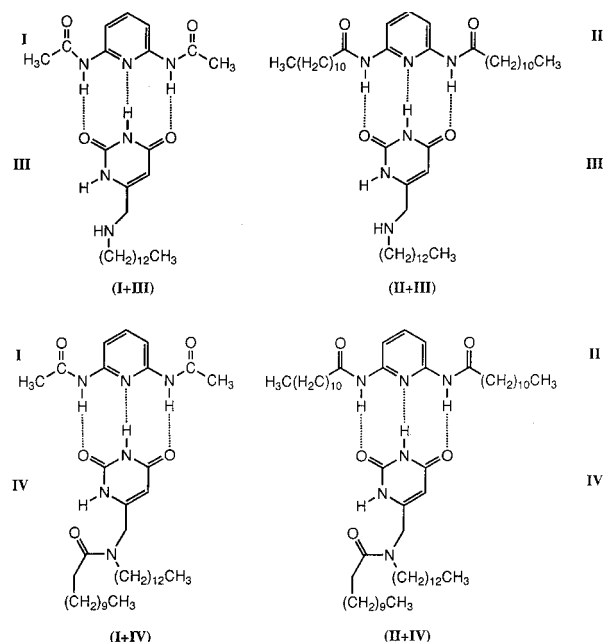
Calculated for 6-(*N*-tridecylundecamido)methyluracil ( $\text{C}_{30}\text{H}_{55}\text{N}_3\text{O}_3$ , **IV**): C, 71.25; H, 10.95; N, 8.30. Found: C, 71.25; H, 10.95; N, 8.95.  $^1\text{H}$  NMR ( $\text{CDCl}_3$ )  $\delta$  0.88 (t, 6H,  $J = 7.0$  Hz), 1.26–1.58 (m, 40H), 2.36 (t, 2H,  $J = 7.8$  Hz), 4.16 (s, 2H), 5.52 (s, 1H), 8.14 (s, 1H), 9.51 (s, 1H).

Cetyltrimethylammonium bromide (CTAB) was used as supplied without further purification, and results of the characterization of this compound are included for comparison. Calculated for CTAB ( $\text{C}_{19}\text{H}_{42}\text{NBr}$ ): C, 62.63; H, 11.53; N, 3.84. Found: C, 62.78; H, 11.60; N, 3.89.  $^1\text{H}$  NMR ( $\text{CDCl}_3$ )  $\delta$  0.88 (t, 3H,  $J = 6.6$  Hz), 1.25–1.36 (m, 28H), 1.78 (m, 2H), 3.50 (s, 9H).

**Self-Assembly of Supermolecules and Heterosupermolecules.** To assemble a supermolecule or heterosupermolecule, the required components were dissolved in  $\text{CDCl}_3$  at room temperature. The resulting complex was characterized by  $^1\text{H}$  NMR and FT-IR spectroscopy.

**Characterization Techniques.** All NMR spectra were recorded using either a JEOL JNM-GX270 FT or Varian 500 FT spectrometer at 20 °C unless otherwise stated. All IR spectra were recorded using a Mattson Galaxy 3000 FT

Scheme 3



spectrometer ( $\text{CaF}_2$  windows, 0.20 mm path length, variable temperature) at 20 °C unless otherwise stated.

## Results and Discussion

We first discuss the characterization of model self-assembled supermolecules by  $^1\text{H}$  NMR and FT-IR spectroscopies. Similar results for model heterosupermolecules are considered. Finally, we consider some future developments and possible applications of these studies.

**I. Characterization of Model Supermolecules by NMR.** Self-assembly of *N,N*-2,6-pyridinediylbis[acetamide] (**I**) or *N,N*-2,6-pyridinediylbis[undecamide] (**II**) and 6-(*N*-tridecylamino)methyluracil (**III**) or 6-(*N*-tridecylundecamido)methyluracil (**IV**) in  $\text{CDCl}_3$  leads to formation of the supermolecules shown in Scheme 3. These 1:1 complexes, denoted (**I+III**) and (**II+III**) or (**I+IV**) and (**II+IV**), respectively, were characterized by  $^1\text{H}$  NMR spectroscopy. We note that these and related supermolecules have previously been prepared by Lehn and co-workers.<sup>9</sup>

Shown in Figure 1 are the  $^1\text{H}$  NMR spectra of **I**, **IV**, and (**I+IV**) in  $\text{CDCl}_3$  (0.004 mol  $\text{dm}^{-3}$ ). The singlet observed for **I** at  $\delta$  7.73 is assigned to the two equivalent amidic protons.<sup>10</sup> The singlets observed for **IV** at  $\delta$  8.97 and 9.53 are assigned to the amidic and imidic protons of the uracil ring.<sup>10</sup> For (**I+IV**), proton resonances are observed at  $\delta$  9.71, 9.88, and 11.83. The resonance at  $\delta$  9.88 clearly correlates, based on a comparison of integrated peak areas, with that of the amidic protons at  $\delta$  7.73 in **I**. The resonances at  $\delta$  9.71 and 11.83 are assumed to correlate with those of the amidic and imidic protons of the uracil ring at  $\delta$  8.97 and 9.53 in **IV**.

Shown in Figure 2 are the  $^1\text{H}$  NMR spectra of **II**, **IV**, and (**II+IV**) in  $\text{CDCl}_3$  (0.004 mol  $\text{dm}^{-3}$ ). The singlet observed for **II** at  $\delta$  7.56 is assigned to the two equivalent amidic protons. The singlets observed for

(8) Kotov, N.; Meldrum, F.; Fendler, J. *J. Phys. Chem.* **1994**, *98*, 8827.

(9) Brienne, M.-J.; Gabard, J.; Lehn, J.-M. *J. Chem. Soc. Chem. Commun.* **1989**, 1868.

(10) (a) Feibush, B.; Fiuroa, A.; Charles, R.; Onan, K.; Feibush, P.; Karger, B. *J. Am. Chem. Soc.* **1986**, *108*, 3310. (b) B. Feibush, M. Saha, Onan, K.; Karger, B.; Giese, R. *J. Am. Chem. Soc.* **1987**, *109*, 7531. (c) Hamilton, A.; Van Engen, D. *J. Am. Chem. Soc.* **1987**, *109*, 5035. (d) Bisson, A.; Carver, F.; Hunter, C.; Waltho, J. *J. Am. Chem. Soc.* **1994**, *116*, 10292.

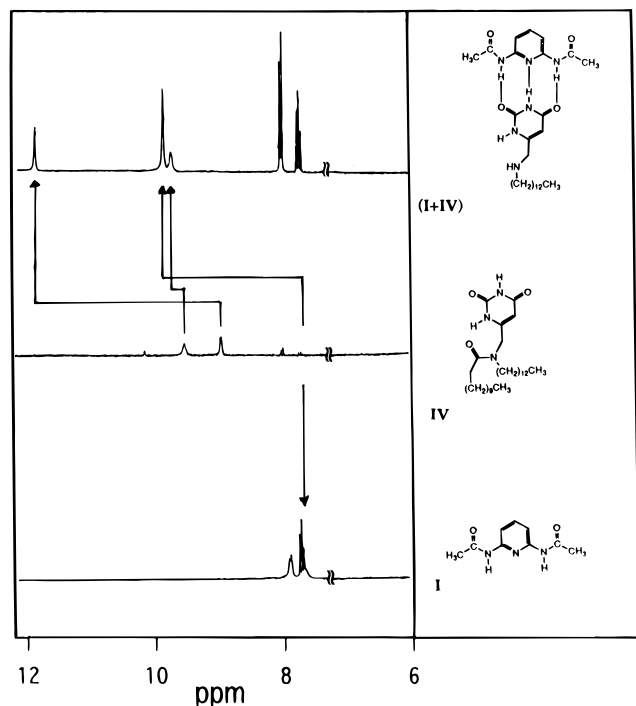


**Figure 1.**  $^1\text{H}$  NMR spectra of  $0.004 \text{ mol dm}^{-3}$  of **I**, **IV**, and **(I+IV)** in  $\text{CDCl}_3$  at  $20^\circ\text{C}$ .

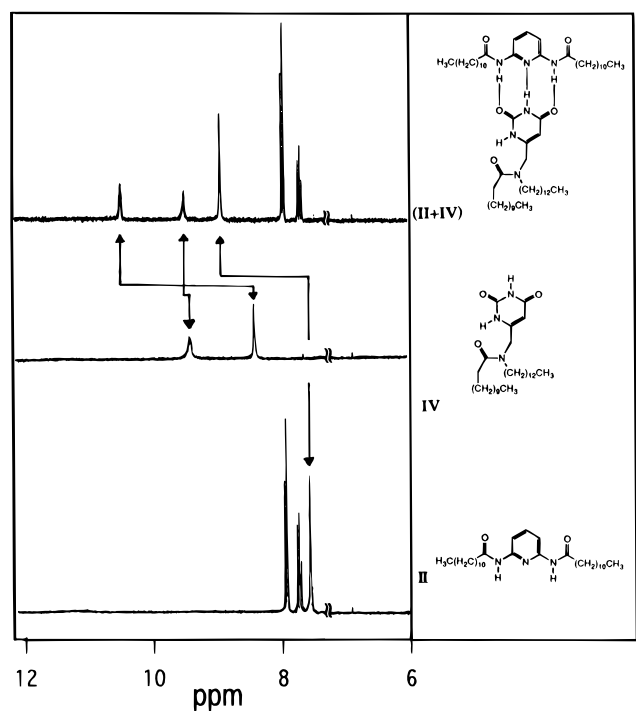


**Figure 2.**  $^1\text{H}$  NMR spectra of  $0.004 \text{ mol dm}^{-3}$  of **II**, **IV**, and **(II+IV)** in  $\text{CDCl}_3$  at  $20^\circ\text{C}$ .

**IV** at  $\delta 8.43$  and  $9.45$  are assigned to the amidic and imidic protons of the uracil ring. For **(II+IV)** the corresponding proton resonances are observed at  $\delta 8.98$ ,  $9.54$ , and  $10.47$ . The resonance at  $\delta 8.98$  clearly correlates, based on a comparison of integrated peak areas, with that of the amidic protons in **II** at  $\delta 7.56$ . The resonances at  $\delta 9.54$  and  $10.47$  are assumed to correlate with those of the amidic and imidic protons of the uracil ring at  $\delta 8.43$  and  $9.45$  in **IV**.

By comparison with previously reported  $^1\text{H}$  NMR studies, it is concluded that the supermolecules **(I+IV)** and **(II+IV)** shown in Scheme 3 are formed by self-

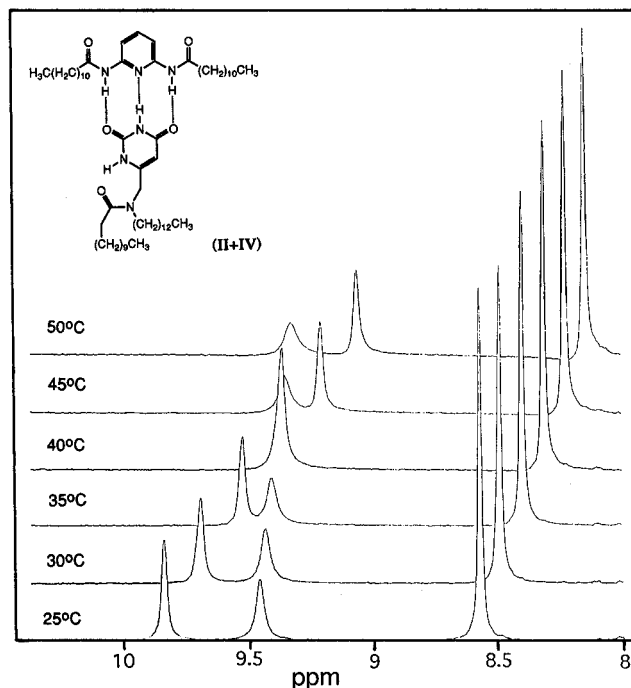


**Figure 3.**  $^1\text{H}$  NMR spectra of  $0.004 \text{ mol dm}^{-3}$  of **(II+IV)** in  $\text{CDCl}_3$  at the indicated temperatures.

assembly.<sup>9,10</sup> It is also concluded, from the results of similar  $^1\text{H}$  NMR studies (not shown), that the supermolecules **(I+III)** and **(II+III)** are formed by self-assembly. We note, however, that assignment of the spectra in Figures 1 and 2 is incomplete, i.e., the amidic and imidic resonances on the uracil ring in **IV** have not been uniquely assigned. Consequently, uncertainty exists as to the exact magnitude of the down-field shift of the uracil ring proton resonances following self-assembly of **(I+IV)** and **(II+IV)** or **(I+III)** and **(II+III)**. Presented below are the results of studies directed toward a complete assignment of the  $^1\text{H}$  NMR spectra for **(II+IV)** in Figure 2.

Shown in Figure 3 are variable-temperature  $^1\text{H}$  NMR spectra of **(II+IV)** between  $25$  and  $50^\circ\text{C}$ . The resonance at  $\delta 8.98$  for **(II+IV)** is observed to shift upfield to  $\delta 8.2$  upon raising the sample temperature to  $50^\circ\text{C}$  and correlates, as expected, with the resonance at  $\delta 7.56$  for **II** in Figure 2. Similarly, the resonance at  $\delta 10.47$  for **(II+IV)** is observed to shift upfield to  $\delta 9.1$  upon raising the sample temperature to  $50^\circ\text{C}$  and correlates with the resonance at  $\delta 8.43$  for **IV** in Figure 2. Finally, the resonance at  $\delta 9.54$  in **(II+IV)** is largely temperature independent, shifting upfield by less than  $0.1$  ppm to  $\delta 9.4$  upon increasing the sample temperature to  $50^\circ\text{C}$ , and correlates with the singlet at  $\delta 9.45$  for **IV** in Figure 2.

These findings support assignment of the resonances at  $\delta 8.98$  and  $10.47$  in **(II+IV)** to intermolecularly hydrogen-bonded protons for the following reasons: First, both resonances exhibit down-field shifts of greater than  $1$  ppm upon formation of **(II+IV)**; second, raising the sample temperature to  $50^\circ\text{C}$  results in both resonances shifting upfield to values close to those observed for the free components. Concerning the proton resonance at  $\delta 9.54$ , as a downfield shift of less than  $0.1$  ppm is observed upon formation of **(II+IV)** and its position is essentially temperature independent, we conclude this proton is not involved in intermolecular

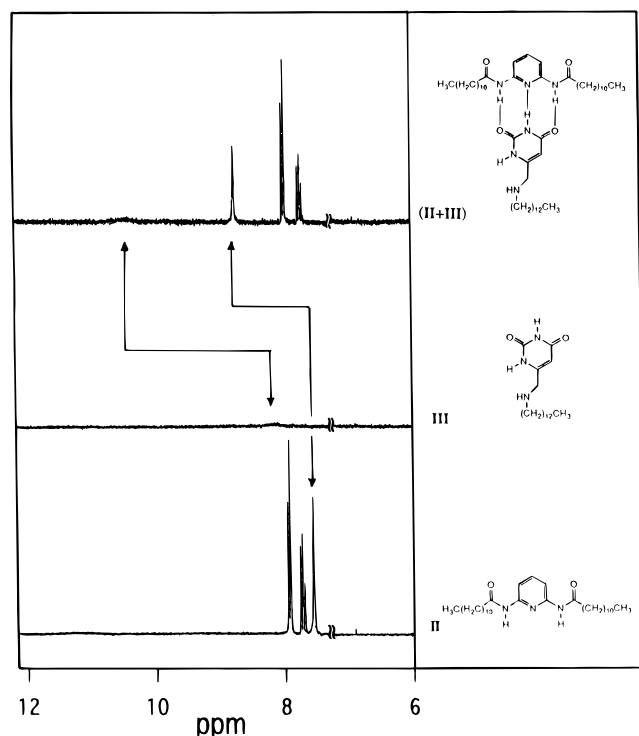


**Figure 4.**  $^1\text{H}$  NMR spectra of  $0.004 \text{ mol dm}^{-3}$  of **II**, **III**, and **(II+III)** in  $\text{CDCl}_3$  at  $20^\circ\text{C}$ .

hydrogen bonding. In short, of the amidic and imidic protons on the uracil ring of **IV**, only that whose resonance is at  $\delta$  8.43 forms an intermolecular hydrogen bond in **(II+IV)**. To be consistent with the proposed structure for **(II+IV)** it is necessary, therefore, that the resonances at  $\delta$  9.45 and 8.43 be assigned to the amidic and imidic protons on the uracil ring of **IV**, respectively.

The above assignments, while consistent with the data presented, are apparently problematic in the following respect: As the amidic proton in the uracil ring in **IV** is, at first glance, less deshielded than the imidic proton, it might seem more reasonable to assign the upfield resonance at  $\delta$  8.43 to the former and the downfield resonance at  $\delta$  9.45 to the latter. This, in turn, would imply that the proposed structure for **(II+IV)** in Scheme 3 is incorrect. However, this difficulty is resolved by proposing formation of intramolecular hydrogen bonds by the amidic proton in **IV** to the oxygen and nitrogen atom lone pairs present in the side chain. Specifically, this would account for the downfield shift of this proton resonance and for the fact that the position of this resonance is largely temperature independent and unaffected by formation of **(II+IV)**.

To test this hypothesis, the  $^1\text{H}$  NMR spectra of **II**, **III**, and **(II+III)** in  $\text{CDCl}_3$  ( $0.004 \text{ mol dm}^{-3}$ ) were recorded; see Figure 4. As above, the singlet observed for **II** at  $\delta$  7.56 is assigned to the two equivalent amidic protons. In the presence of only a single suitable hydrogen-bond acceptor in the side chain of **III**, namely, the nitrogen atom lone pair, a broad two-proton resonance is observed at  $\delta$  8.2. The latter is assigned to the amidic and imidic protons of the uracil ring. The near equivalence of these two protons is likely a consequence of their facile exchange.<sup>10</sup> For **(II+III)** a two proton resonance at  $\delta$  8.72 and a broad one-proton resonance at  $\delta$  10.5 are observed. The resonance at  $\delta$  8.72 is assigned to the hydrogen-bonded amidic protons of **II**. The reso-

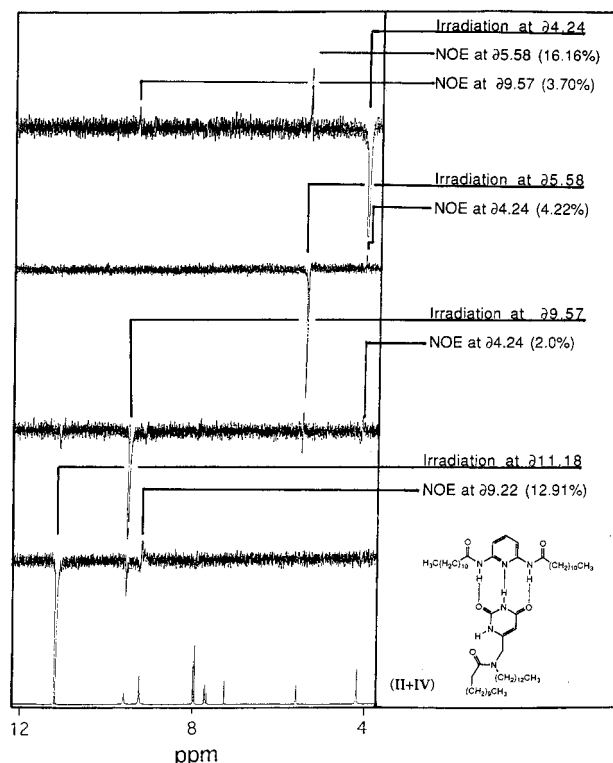
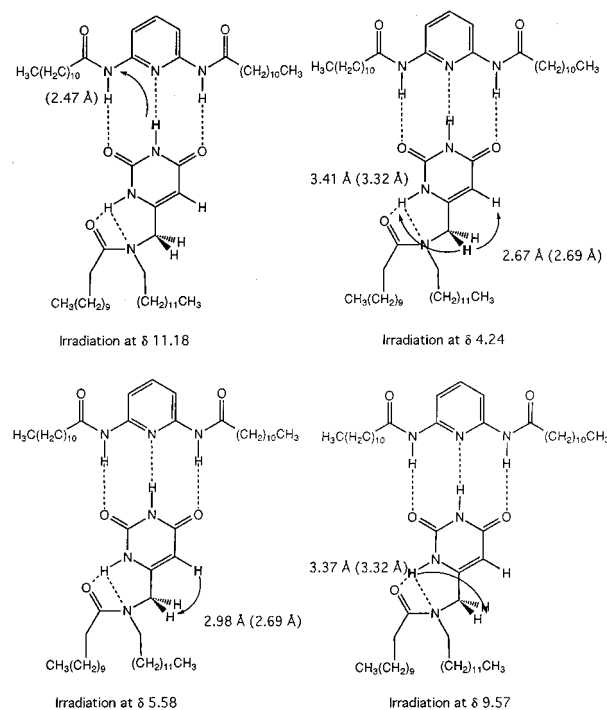


**Figure 5.**  $^1\text{H}$  difference NOE spectra of  $0.004 \text{ mol dm}^{-3}$  of **(II+IV)** in  $\text{CDCl}_3$  at  $20^\circ\text{C}$ .

#### Scheme 4



nances at  $\delta$  10.5 is assigned to the hydrogen-bonded imidic proton of **III**. An additional one-proton resonance that might be assigned to the free amidic proton of **III** is not observed. It is assumed that this is due to a simultaneous broadening and upfield shift of this resonance in the absence of a second suitable hydrogen-bond acceptor, namely, the oxygen atom lone pair.

To further test this hypothesis a series of difference NOE experiments were performed for **II**, **IV**, and **(II+IV)**. Shown in Figure 5 are the results of these

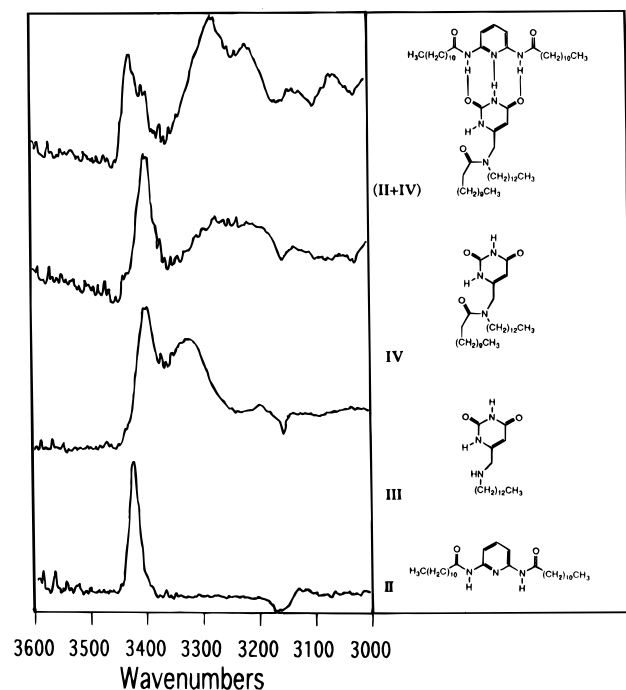


**Figure 6.** FT-IR spectra of 0.004 mol dm<sup>-3</sup> of **II**, **III**, **IV**, and **(II+IV)** in CDCl<sub>3</sub> at 20 °C.

experiments for **(II+IV)**. Upon saturating the resonance at  $\delta$  4.24, positive NOEs at  $\delta$  5.58 (8.08%, normalized for one proton) and  $\delta$  9.57 (1.85%, normalized for one proton) were observed. Upon saturating the resonance at  $\delta$  5.58, a positive NOE at  $\delta$  4.24 (4.22%) was observed. Upon saturating the resonance at  $\delta$  9.57, a positive NOE at  $\delta$  4.24 (2.0%) was observed. Upon saturating the resonance at  $\delta$  11.18, a positive NOE at  $\delta$  9.22 (12.91%) was observed. We note the existence of negative NOEs between the amidic and imidic protons on the uracil ring, these being assigned to exchange of the above protons.

The above NOEs are consistent with the structure for **IV** in **(II+IV)** shown in Scheme 4.<sup>11</sup> Specifically, the relative interatomic distances calculated from the NOE spectra in Figure 5 are in good agreement with those derived from the energy-minimized structure in Scheme 4. The structure in question being stabilized by the formation of two intramolecular hydrogen bonds by the amidic proton on the uracil ring to the lone pairs on the oxygen and nitrogen atoms of the side chain in **IV**. These findings strongly support the assertion that the amidic proton of the uracil ring is intramolecularly hydrogen bonded and is, as a consequence, shifted downfield of the imidic proton on the uracil ring. The existence of these intramolecular hydrogen bonds also accounts for the invariance of the resonance at  $\delta$  9.57 to formation of the 1:1 complex **(I+IV)** and temperature variation.

Taken together, the results of the <sup>1</sup>H NMR studies presented above strongly support the structures originally proposed for the supermolecules in Scheme 3.<sup>9,10</sup> However, these studies also significantly extend the evidence supporting the proposed structures and, apparently for the first time, permit a full assignment of the measured <sup>1</sup>H NMR spectra.

**II. Characterization of Model Supermolecules by FT-IR.** The ultimate objective of these studies is to characterize structures similar to that shown in Scheme

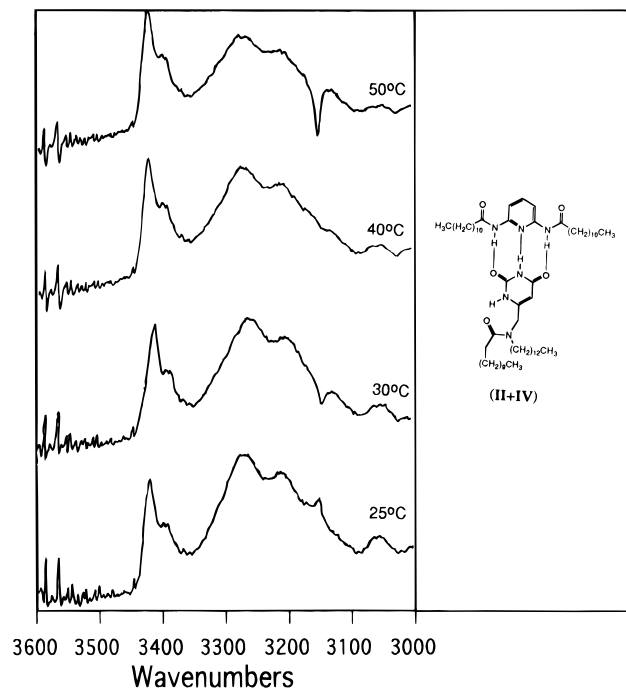


**Figure 7.** FT-IR spectra of 0.004 mol dm<sup>-3</sup> of **(II+IV)** in CDCl<sub>3</sub> at the indicated temperatures.

2; consequently, the supermolecules in Scheme 3 were also characterized by IR spectroscopy. This approach, it was hoped, would permit structural characterization of complexes containing semiconductor nanocrystallites where application of a full range of NMR techniques was not possible. As above, we report our findings in detail for **(II+IV)**.

Shown in Figure 6 are the FT-IR spectra of **II**, **III**, **IV**, and **(II+IV)** in CDCl<sub>3</sub> (0.004 mol dm<sup>-3</sup>). The absorbance band observed for **II** at 3423 cm<sup>-1</sup> may readily be assigned to the -NH stretch of the amino groups.<sup>12,13</sup> For **IV** we observe bands at 3395 and 3250 cm<sup>-1</sup> (broad) that may be assigned to the -NH stretches of the imidic and amidic protons respectively.<sup>12-14</sup> The amidic band is broadened and shifted to lower frequencies by formation of an intramolecular hydrogen bond; see Scheme 4. This latter assignment is supported by comparison with the spectrum measured for **III** where formation of an intramolecular hydrogen bond is not observed. Correspondingly, two relatively sharp bands are observed at 3395 and 3325 cm<sup>-1</sup> assigned to the imidic and amidic protons of the uracil ring, respectively.

Upon mixing equimolar quantities of **II** and **IV** the following spectral changes were noted: The absorption bands at 3423 and 3395 cm<sup>-1</sup> are reduced in intensity; the absorption band at 3250 cm<sup>-1</sup> is unchanged in intensity; and finally, series of bands at 3276, 3209, and

(11) Calculation of an energy-minimized structure for **(II+IV)** in Scheme 4 was performed using the PCMODEL (MMX force field) program. The distance between the amidic proton on **II** and the imidic proton on the uracil ring of **IV** in **(II+IV)** was used as the basis for prediction of the interatomic distances from the measured NOE spectra; see Scheme 4. The interatomic distances derived from the energy-minimized structure are given in brackets for comparison.

(12) Bellamy, L. J. *The Infrared Spectra of Complex Molecules*; Mathuen: London, 1954.

(13) Pimentel, G.; Mc Clellan, A. *The Hydrogen Bond*; Freeman: San Francisco, 1956.

(14) (a) Tsuboi, M. *Appl. Spectrosc. Rev.* **1969**, 3, 45. (b) Susi, H.; Ard, J. *Spectrochim. Acta* **1971**, 27A, 1549.

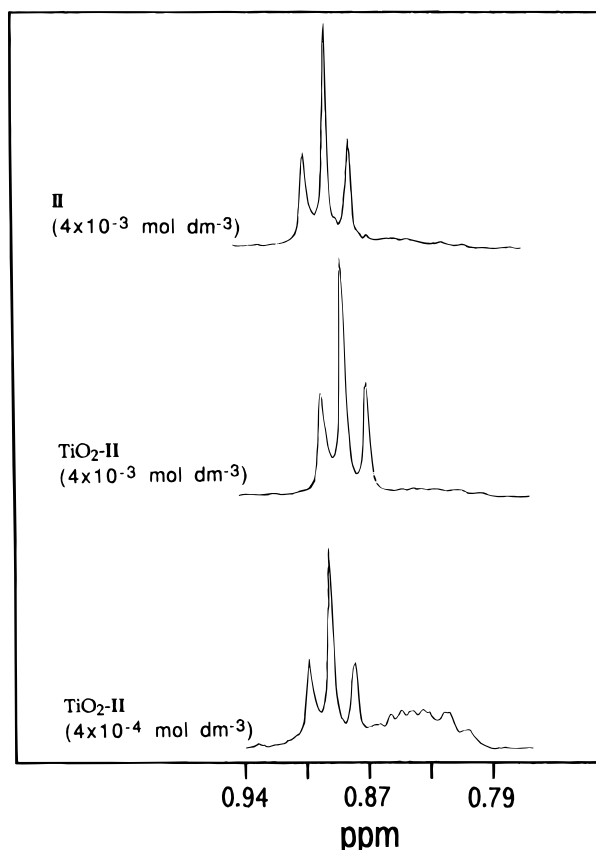


**Figure 8.**  $^1\text{H}$  NMR spectra of **II** and  $(\text{TiO}_2)\text{-II}$  in  $\text{CDCl}_3$  at  $20^\circ\text{C}$ . The concentration of  $\text{TiO}_2$  nanocrystallites is  $4 \times 10^{-7} \text{ mol dm}^{-3}$ . The concentration of **II** is as indicated.

$3063 \text{ cm}^{-1}$  are newly observed. The reduced intensity of the bands at  $3423 \text{ cm}^{-1}$  for **II** and  $3395 \text{ cm}^{-1}$  for **IV** is consistent with their assignment to the two equivalent amidic protons in **II** and the imidic proton of the uracil ring in **IV**, respectively. The fact that the band  $3250 \text{ cm}^{-1}$ , unlike those at  $3423$  and  $3395 \text{ cm}^{-1}$ , shows no reduction in intensity upon formation of  $(\text{II}+\text{IV})$  is consistent with assignment of this absorption to the intramolecularly hydrogen-bonded amidic proton of the uracil ring. The newly observed absorbances are assigned to hydrogen bonded  $-\text{NH}$  stretches in  $(\text{II}+\text{IV})$ .<sup>15</sup>

To further support the above assignments FT-IR spectra of **II**, **IV**, and  $(\text{II}+\text{IV})$  in  $\text{CDCl}_3$  ( $0.004 \text{ mol dm}^{-3}$ ) were recorded at temperatures between  $25$  and  $50^\circ\text{C}$ . The results for  $(\text{II}+\text{IV})$  are shown in Figure 7. Consistent with the above assignments, the intensity of the absorption bands at  $3423$  and  $3395 \text{ cm}^{-1}$  exhibit increased intensities at elevated temperatures. As expected, the intensity of the absorption bands  $3250 \text{ cm}^{-1}$  assigned to the intramolecular hydrogen-bonded amidic proton, shows no significant temperature dependence over the measured range. Finally, the absorption bands at  $3276$ ,  $3209$ , and  $3063 \text{ cm}^{-1}$  decrease in intensity at elevated temperatures, consistent with their assignment to intermolecularly bonded amidic and imidic protons.

These observations are fully consistent with the structural assignments based on the  $^1\text{H}$  NMR spectra

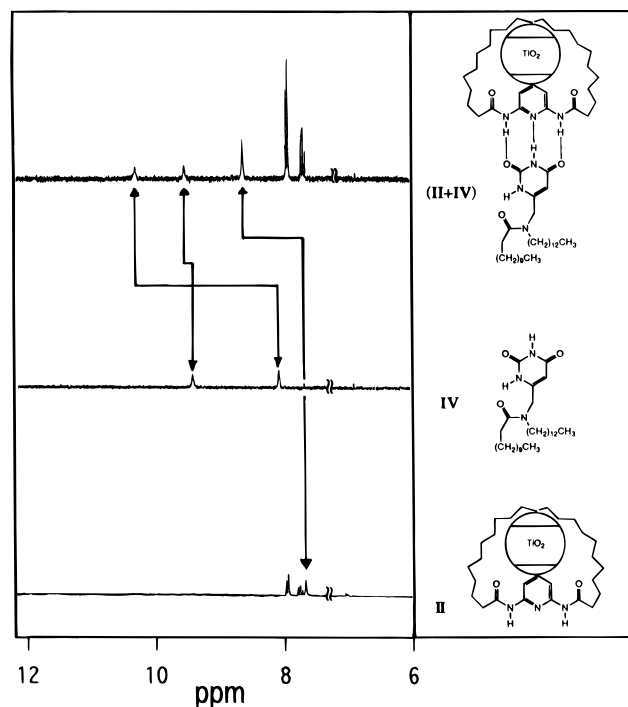


**Figure 9.**  $^1\text{H}$  NMR spectra of  $(\text{TiO}_2)\text{-II}$ , **IV**, and  $(\text{TiO}_2)\text{-(II+IV)}$  in  $\text{CDCl}_3$  at  $20^\circ\text{C}$ . The concentration of  $\text{TiO}_2$  nanocrystallites is  $4 \times 10^{-7} \text{ mol dm}^{-3}$  and that of **II** and **IV** is  $0.004 \text{ mol dm}^{-3}$ .

discussed above for  $(\text{II}+\text{IV})$ . Consequently, FT-IR spectra appear to provide a sound basis on which the formation supermolecules such as those in Scheme 3 may be demonstrated.

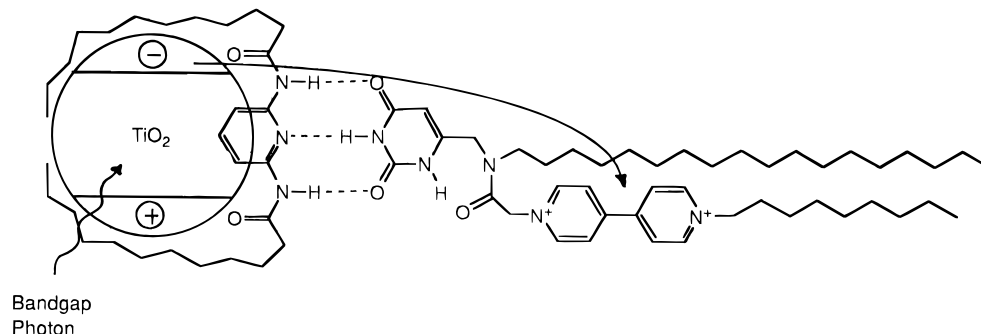
**III. Characterization of Model Heterosupermolecules by NMR and FT-IR.**  $\text{TiO}_2$  nanocrystallites were prepared, following the method of Kotov et al., by arrested hydrolysis of titanium tetraisopropoxide in  $\text{CDCl}_3$  in the presence of added **II** or CTAB.<sup>8</sup> The concentration of added stabilizer was  $0.004 \text{ mol dm}^{-3}$  in each case. The resulting sols, denoted  $(\text{TiO}_2)\text{-II}$  and  $(\text{TiO}_2)\text{-CTAB}$ , respectively, were characterized by UV-vis absorption spectroscopy and by transmission electron microscopy (TEM). The observed onsets for absorption and average crystallite diameters of  $360 \text{ nm}$  and  $22 \pm 2 \text{ \AA}$ , respectively, are in good agreement with the reported values. The nanocrystallite concentration, for both  $(\text{TiO}_2)\text{-II}$  and  $(\text{TiO}_2)\text{-CTAB}$ , was calculated to be  $4 \times 10^{-7} \text{ mol dm}^{-3}$ .

The issue of to what extent **II** interacts with the surface of the  $\text{TiO}_2$  nanocrystallites in  $(\text{TiO}_2)\text{-II}$  is important. Qualitatively, since the above nanocrystallites were prepared in the presence of **II** as a stabilizer and since the resulting sol is as stable as that prepared in the presence of a conventional stabilizer such as CTAB, it may be assumed some fraction of **II** is associated directly with the surface of the dispersed nanocrystallites. We note also, and in support of this view, that the absence of added **II** or CTAB results in a  $\text{TiO}_2$  sol that is highly scattering and unstable over a period of minutes.

More quantitatively, high resolution  $^1\text{H}$  NMR spectra of **II** have been measured. The following resonances are observed for the alkane side chains in **II**:  $\delta$  0.88 ( $\text{CH}_3$ -);  $1.24\text{--}1.27$  ( $-(\text{CH}_2)_8-$ ),  $1.75$  and  $2.36$  ( $-\text{CH}_2-\text{C}(=\text{O})-$ ). Similar spectra have been measured for  $(\text{TiO}_2)\text{-II}$ , and observed is an additional resonance  $0.1$

(15) (a) Hamlin, R.; Lord, R.; Rich, A. *Science* **1965**, *148*, 1734. (b) Kyogoku, Y.; Lord, R.; Rich, A. *Proc. Natl. Acad. Sci. U.S.A.* **1967**, *57*, 250. (c) Kyogoku, Y.; Lord, R.; Rich, A. *J. Am. Chem. Soc.* **1967**, *89*, 496. (d) Kyogoku, Y.; Lord, R.; Rich, A. *Biochim. Biophys. Acta* **1969**, *179*, 10. (e) Zundel, G.; Lubos, W.; Kolkenbeck, K. *Can. J. Chem.* **1971**, *49*, 3795.

Scheme 5



ppm upfield of that at  $\delta$  0.88 ( $\text{CH}_3^-$ ). This resonance is assigned to alkane chains adsorbed at the surface of a  $\text{TiO}_2$  nanocrystallite.<sup>16</sup> From the integrated peak areas it is estimated that about half of **II** are at the surface of a  $\text{TiO}_2$  nanocrystallite in  $(\text{TiO}_2)\text{-II}$ ; see Figure 8. These experiments were repeated for  $(\text{TiO}_2)\text{-II}$  prepared using one-tenth of the concentration of **II** ( $0.0004 \text{ mol dm}^{-3}$  in  $\text{CDCl}_3$ ). As above, a new resonance was observed about 0.1 ppm upfield of that at  $\delta$  0.88 ( $\text{CH}_3^-$ ). From the integrated peak areas it is estimated that greater than two-thirds of **II** are at the surface of a  $\text{TiO}_2$  nanocrystallite. It should be noted that other more complex spectral changes are observed for the resonances at  $\delta$  1.24–1.27, 1.75, and 2.36 and that these are the subject of a detailed study at the present time.

Following addition of **IV** ( $0.004 \text{ mol dm}^{-3}$ ) to  $(\text{TiO}_2)\text{-II}$ , it was expected **IV** would associate with  $(\text{TiO}_2)\text{-II}$  by complementary hydrogen bonding as shown in Scheme 2. The resulting heterosupramolecule to be denoted  $(\text{TiO}_2)\text{-(II+IV)}$ . In the case of  $(\text{TiO}_2)\text{-CTAB}$ , no such interaction was expected. Detailed characterization of  $(\text{TiO}_2)\text{-II}$  and  $(\text{TiO}_2)\text{-CTAB}$  by  $^1\text{H}$  NMR and FT-IR spectroscopy was undertaken prior to and following addition of **IV** to test the above expectations. We note such detailed characterization is possible largely as a consequence of the detailed spectroscopic studies reported above for the model supramolecular systems in Scheme 3.

Shown in Figure 9 are the  $^1\text{H}$  NMR spectra of  $(\text{TiO}_2)\text{-II}$ , **IV**, and  $(\text{TiO}_2)\text{-(II+IV)}$  in  $\text{CDCl}_3$ . The  $^1\text{H}$  NMR spectrum of  $(\text{TiO}_2)\text{-II}$  is in good agreement with that observed above for **II**; see Figure 2. Specifically, the resonance observed at  $\delta$  7.68 is assigned to the two equivalent the amidic protons of **II**. The  $^1\text{H}$  NMR spectrum of **IV**, with the imidic and amidic proton resonances of the uracil ring at  $\delta$  8.14 and 9.44, respectively, is also in good agreement with that observed above for **IV**; see Figure 2. Following addition of **IV** to  $(\text{TiO}_2)\text{-II}$ , proton resonances are observed at  $\delta$  8.51, 9.54, and 11.1. The resonance at  $\delta$  8.51 is assigned, based on a comparison of integrated peak areas and by comparison with  $(\text{II+IV})$ , to the intermolecularly hydrogen-bonded amidic protons on **II**. The resonances at  $\delta$  9.54 and 11.1 are assigned, also by comparison with  $(\text{II+IV})$ , to the intramolecularly hy-

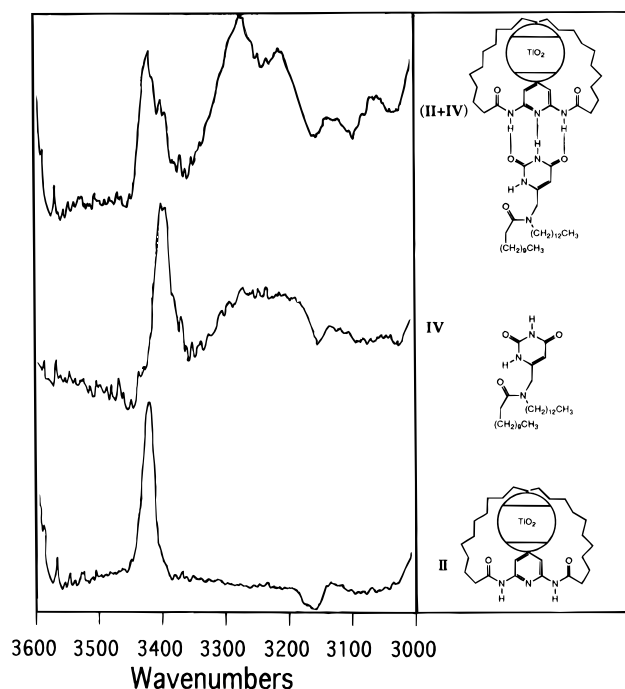


**Figure 10.** FT-IR spectra of  $(\text{TiO}_2)\text{-II}$ , **IV**, and  $(\text{TiO}_2)\text{-(II+IV)}$  in  $\text{CDCl}_3$  at  $20^\circ\text{C}$ . The concentration of  $\text{TiO}_2$  nanocrystallites is  $4 \times 10^{-7} \text{ mol dm}^{-3}$  and that of **II** and **IV** is  $0.004 \text{ mol dm}^{-3}$ .

drogen-bonded amidic and intermolecularly hydrogen-bonded imidic proton of **IV**. In short, the  $^1\text{H}$  NMR spectra in Figure 9 are entirely consistent with association of  $(\text{TiO}_2)\text{-II}$  and **IV** by complementary hydrogen bonding to form the 1:1 heterosupramolecular complex shown in Scheme 2. It should be noted that on a few occasions no resonance was observed at  $\delta$  9.54 that could be assigned to an intramolecularly hydrogen-bonded amidic peak, as was the case for  $(\text{II+IV})$ . This, it is suggested, is likely due to preferential interaction of the oxygen of the alkane side chain with the surface of a  $\text{TiO}_2$  nanocrystallite.<sup>17</sup> As a consequence, the intramolecular hydrogen bond observed in  $(\text{II+IV})$  is not formed and results in a simultaneous broadening and upfield shift of this resonance; see discussion above of spectra of  $(\text{II+III})$ .

Shown in Figure 10 are the FT-IR spectra of  $(\text{TiO}_2)\text{-II}$ , **IV**, and  $(\text{TiO}_2)\text{-(II+IV)}$  in  $\text{CDCl}_3$ . These spectra further support a view that  $(\text{TiO}_2)\text{-II}$  and **IV** form the heterosupramolecule  $(\text{TiO}_2)\text{-(II+IV)}$  by complementary hydrogen bonding. It is noted that the spectra of  $(\text{TiO}_2)\text{-II}$  and **IV** are in excellent agreement with those of **II** and **IV** shown in Figure 6. Further, the spectrum for  $(\text{TiO}_2)\text{-(II+IV)}$  is in excellent agreement with that

(16) Halaoui, L.; Kehr, S.; Lube, M.; Aubuchon, S.; Hagan, C.; Wells, R.; Coury, L. *Synthesis, Characterisation and Immobilisation of Nanocrystalline Binary and Ternary III–V (13–15) Compound Semiconductors*; ACS Symposium Series, *Nanotechnology: Molecularly Designed Materials*; Chow, G.-M., Gonsalves, K., Eds.; American Chemical Society: Washington, DC, 1996; Vol. 622, Chapter 12,

observed for (**II**+**IV**); see also Figure 6. Specifically, the absorption bands at 3423 and 3395  $\text{cm}^{-1}$  are reduced in intensity, the intensity of the absorption band at 3250  $\text{cm}^{-1}$  remains unchanged, while absorption bands at 3276, 3210, and 3065  $\text{cm}^{-1}$  are newly observed. As discussed above for (**II**+**IV**), these spectral changes are consistent with formation of the hydrogen bonded complex shown in Scheme 2.

To further increase confidence in the above assignments,  $^1\text{H}$  NMR and FT-IR spectra were recorded for  $(\text{TiO}_2)$ -CTAB, **IV** and 1:1 mixtures of  $(\text{TiO}_2)$ -CTAB and **IV** in  $\text{CDCl}_3$ . Briefly, there is no evidence to suggest formation of a hydrogen-bonded complex similar to  $(\text{TiO}_2)$ -(**II**+**IV**). Specifically, no downfield shift is observed for the proton resonances of **IV** in a 1:1 mixture of  $(\text{TiO}_2)$ -CTAB and **IV**. For FT-IR spectra measured under similar conditions, no additional absorbances that could be assigned to hydrogen-bonded protons in **IV** are observed between 3400 and 3000  $\text{cm}^{-1}$ .

**IV. Future Work.** The above studies establish that it is possible, by use of appropriately modified stabilizers, to prepare  $\text{TiO}_2$  nanocrystallites capable of selectively binding an appropriate molecular substrate. The heterosupramolecule thus formed may be characterized by  $^1\text{H}$  NMR and FT-IR studies.

In a development of these studies a series of heterosupramolecules similar to the one shown in Scheme 5

have been prepared.<sup>18</sup> Here an appropriately stabilized  $\text{TiO}_2$  nanocrystallite selectively binds a molecular substrate containing an electron acceptor, specifically viologen. Bandgap excitation of the  $\text{TiO}_2$  nanocrystallite results in electron transfer to the viologen molecule adsorbed, by complementary hydrogen bonding, at the crystallite surface. These studies will be reported soon.<sup>18</sup>

Potential applications of these studies include the self-assembly and self-organization of molecular devices containing both condensed phase and molecular components. The general advantages of this approach, principally greater functional diversity and capacity for function modulation, have been discussed in detail elsewhere.<sup>7</sup>

**Acknowledgment.** We thank Prof. Brienne for providing us with a detailed description of the preparation of the molecules used in the present study. This work was supported in part by a grant from the Commission of the European Union under the Joule II program (Contract JOU2-CT93-0356) and in part by a grant from Forbairt (Contract SC-95-203).

CM9604470

(17) Moser, J.; Punchihewa, S.; Infelta, P.; Grätzel, M. *Langmuir* **1991**, *7*, 3012.

(18) Cusack, L.; Rao, S. N.; Fitzmaurice, D., manuscript in preparation.